

Article

Enigmatic Alluvial Sapphires from the Orosmayo Region, Jujuy Province, Northwest Argentina: Insights into Their Origin from in situ Oxygen Isotopes

Ian T. Graham ^{1,*} , Stephen J. Harris ¹, Laure Martin ², Angela Lay ¹ and Eduardo Zappettini ³

¹ PANGEA Research Centre, School of Biological, Earth and Environmental Sciences, University of NSW, Sydney 2052, Australia

² Centre for Microscopy Characterisation and Analysis, The University of Western Australia, Perth 6009, Australia

³ Argentine Geological-Mining Survey (SEGEMAR), Buenos Aires C1067ABB, Argentina

* Correspondence: i.graham@unsw.edu.au; Tel.: +61-435-4296-445

Received: 21 May 2019; Accepted: 25 June 2019; Published: 27 June 2019



Abstract: This study sought to investigate in situ oxygen isotopes ($\delta^{18}\text{O}$) within alluvial colorless-white to blue sapphires from the Orosmayo region, Jujuy Province, NW Argentina, in order to provide additional constraints on their origin and most likely primary geological environment. Analyses were conducted using the in situ SIMS oxygen isotope technique on the same grains that were analyzed for their mineral inclusions and major and trace element geochemistry using EMPA and LA-ICP-MS methods in our previous study. Results show a significant range in $\delta^{18}\text{O}$ across the suite, from +4.1‰ to +11.2‰. Additionally, akin to their trace element chemistry, there is significant variation in $\delta^{18}\text{O}$ within individual grains, reaching a maximum of 1.6‰. Both the previous analyses and $\delta^{18}\text{O}$ results from this study suggest that these sapphires crystallized within the lower crust regime, involving a complex interplay of mantle-derived lamprophyres and carbonatites with crustal felsic rocks and both mantle- and crustal-derived metasomatic fluids. This study reinforces the importance of the in situ analysis of gem corundums, due to potential significant variation in major and trace element chemistry and ratios and even oxygen isotope ratios within discrete zones in individual grains.

Keywords: sapphires; corundum; in situ oxygen isotopes; Orosmayo Argentina; lamprophyre; secondary ion mass spectrometry (SIMS); carbonatite

1. Introduction

Since the seminal paper of Giuliani et al. (2005) [1], oxygen isotopes have been widely used in order to help constrain the likely geological environment of formation for gem sapphires and rubies, especially those from alluvial deposits whose primary formation is unknown [1–5], such as in the case of the sapphires from this study.

Although worldwide corundum oxygen isotope values cover a wide range from -27‰ (Khitostrov, Russia) to $+23\text{‰}$ (Mong Hsu, Myanmar), most are in the range of $+3\text{‰}$ to $+21\text{‰}$ [1,3,6–9]. This criterion has often been used to determine the geological origin of colored corundum, and especially the gem corundums, rubies and sapphires. However, there are only a few studies on in situ oxygen isotope analysis of gem corundums [10,11]. The next research frontier is the use of in situ oxygen isotopic compositions combined with detailed LA-ICP-MS and multivariate statistical methods to help “fingerprint” the geographic location (i.e., geographic typing) of gem corundums.

As there are a number of possible geological environments for gem corundum formation [3], any information which can help provide constraints on their origin is of great use. Trace element geochemistry of gem corundums has been widely used for this in the past, especially when distinct and/or unusual chemistry can provide even site-specific signatures useful for geographic typing [10–13].

In this study, we investigated the primary origin of the little-known alluvial colorless-white to blue sapphires from the Orosmayo region, Jujuy Province, NW Argentina using in situ oxygen isotope analysis. The discovery of alluvial sapphires in this region of NW Argentina dates back to 1991 during the exploration for alluvial gold in the Orosmayo region. These sapphires were first described by Zappettini and Mutti (1997) [14], and then in a more detailed study on the sapphires themselves by Harris et al. (2017) [15] using SEM, EMPA, and LA-ICP-MS techniques. A summary of the main findings of Harris et al. (2017) [15] is given in Table 1.

Table 1. Summary of main findings of Harris et al. (2017) [15] for the Orosmayo sapphire suite (bdl= below detection limit).

Color range	white, pale to deep blue, pale lilac, pale pink
Color distribution	oscillatory, sector (most common), star sapphires
Surface features	percussion marks, corrosion features
Mineral Inclusions	apatite, rutile, magnetite, phlogopite, trikalsilite, pyrite, baryte, monazite-(La), xenotime-(Y), zircon
Ga/Mg	0.3–10.4
Fe/Mg	4–117
Ti	47–8670
V	15–399
Cr	bdl-506
Ga	38–239
Mg	11–253
Elevated trace elements	Si, P, Ca, Y, La, Ce, Nd, Zn, Pb, Be, Nb, Ta, Sn, Th, U

Orosmayo (located at approximately 22°15' S–66°25' W) is located on the western slope of the Sierra de Rinconada, Jujuy Province, within the San Juan de Oro Basin of northwest Argentina (Figure 1; [14,15]). The area forms part of the *Puna* of northwestern Argentina which connects with the Altiplano of Bolivia to form a plateau [14,16]. The sapphires were sampled from stream sediments located at approximately 22°30' S and 66°30' W (see Harris et al. 2017; [15]).

2. Materials and Methods

The same exact grain mounts used in the previous study of Harris et al. (2017) [15] were also used in this study with the addition of a standard (PAR-1; see Wang et al. 2019 [11]), which was embedded into each polished mount before they were then repolished. This study analyzed 16 sapphire grains (AC-1 through to AC-16) obtained from the 37 original grains analyzed by Zappettini and Mutti (1997) [14]. The sapphires from this region range in size from a few mm up to 10 mm and all represent a single group in terms of their overall morphology and colors. However, for this study, the smaller grains were used in order to analyze as many grains as possible. The selected grains were mounted in two epoxy discs, with eight grains on each disc, and polished prior to analysis.

Secondary Ionization Mass Spectrometry (SIMS)

The oxygen isotope analyses were made using secondary ion mass spectrometry (SIMS) for the analysis of different areas of selected sapphire grains in situ to measure oxygen isotope ratios with per mil (‰) level precision. For this technique, oxygen ($^{18}\text{O}/^{16}\text{O}$) isotope ratios were analyzed using a Cameca IMS 1280 multi-collector ion microprobe within the Centre for Microscopy, Characterisation and Analysis (CMCA), University of Western Australia (UWA). The materials examined included the 16 variously colored and zoned sapphire grains (AC-1 to AC-16), which were embedded in the middle of one-inch-diameter resin mounts and polished flat. Results were calibrated using the standard PAR-1

of Wang et al. 2019 [11] embedded in a separate mount and measured before and after unknown mounts. Each analysis point is clearly marked on the sample images (Figure 2a,b).

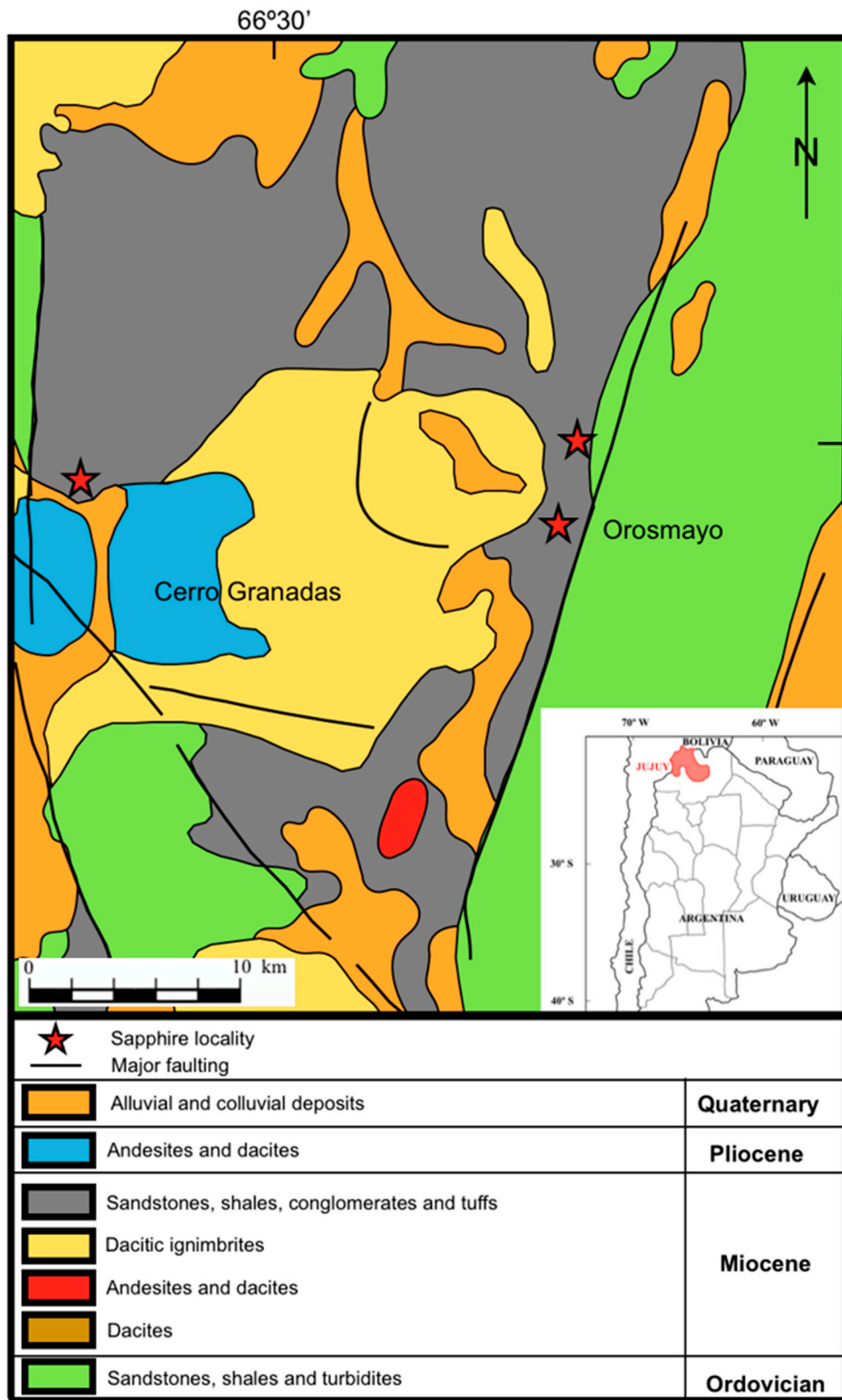
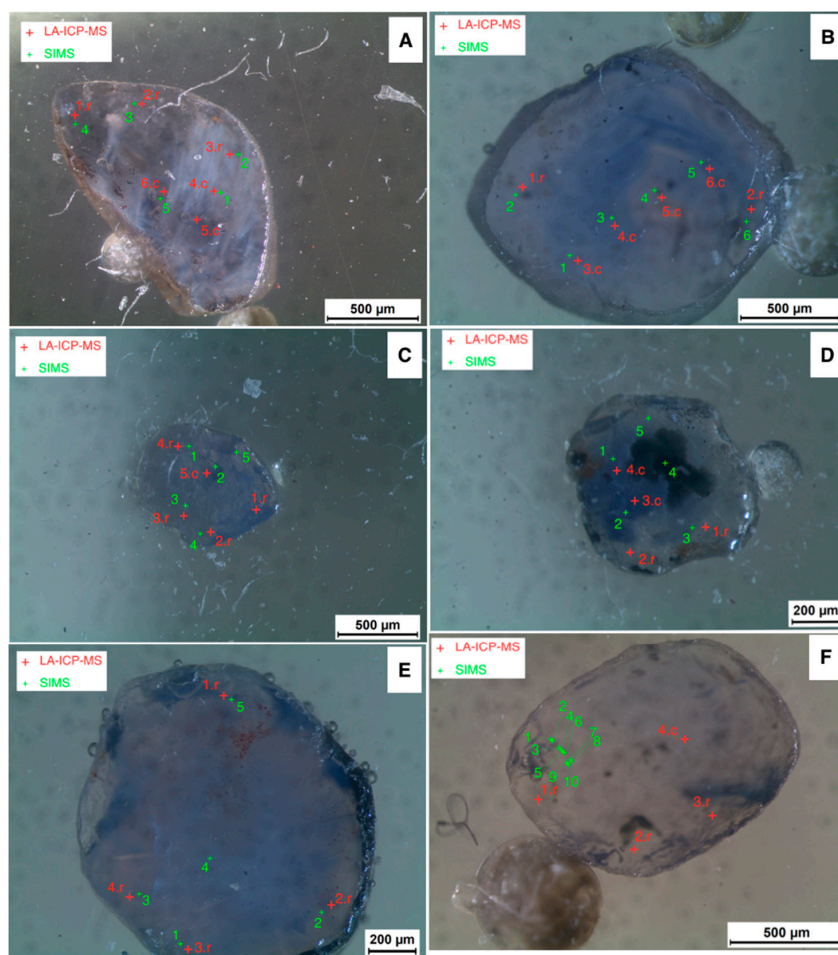


Figure 1. Map showing the location of Orosmayo in northwest Argentina (adapted from Harris et al. 2017) [15].

The sample mounts were carefully cleaned with detergent, distilled water, and ethanol in an ultrasonic bath and then coated with gold (30 nm in thickness) prior to SIMS O isotope analysis. For the oxygen isotopic analyses, secondary ions were sputtered from the sample by bombarding its surface with a Gaussian Cs⁺ beam and a total impact energy of 20 keV. The surface of the sample was rastered with a 2.5 nA primary beam over a 15 × 15 μm area. An electron gun was used to ensure charge compensation during the analyses. Secondary ions were admitted in the double focusing mass spectrometer within a 100 μm entrance slit and focused in the center of a 4000 μm field aperture (100× magnification). They were energy-filtered using a 30 eV band pass with a 5 eV gap towards the high-energy side. ¹⁶O and ¹⁸O were collected simultaneously in multicollection mode in Faraday Cup detectors fitted with 10¹⁰ Ω and 10¹¹ Ω, respectively. Each analysis included pre-sputtering over a 20 μm × 20 μm area for 30 s, and the automatic centering of the secondary ions in the field aperture, contrast aperture, and entrance slit, and consisted of 20 four-second cycles which give an average internal precision of ~0.16‰ (2 standard error (SE)).

External reproducibility during the analytical sessions was evaluated by repeating analyses in one single fragment of PAR-1. External reproducibility in this fragment was 0.3‰ and 0.4‰ (2σ) during the analytical sessions.



(a)

Figure 2. Cont.

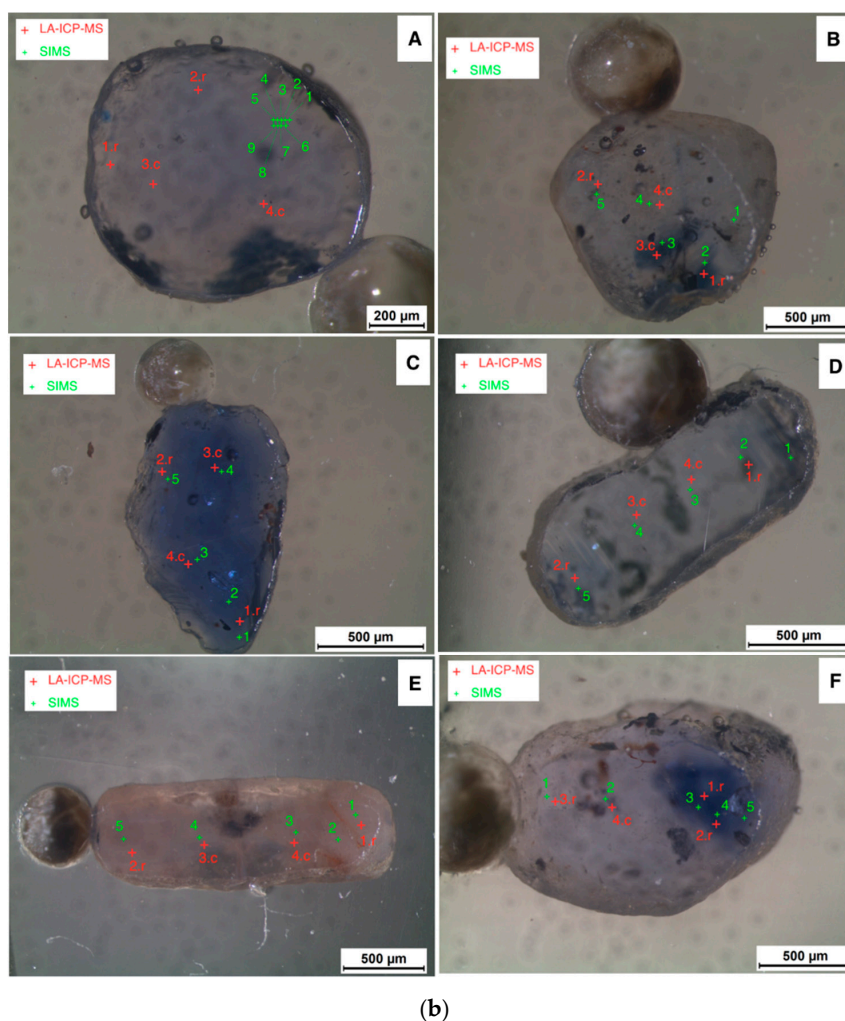


Figure 2. Images of the analyzed sapphires with both LA-ICP-MS and SIMS analysis spots indicated (a). A = AC-1, B = AC-2, C = AC-3, D = AC-4, E = AC-5 and F = AC-7. (b) A = AC-10, B = AC-11, C = AC-13, D = AC-14, E = AC-15 and F = AC-16.

3. Results

The high precision of oxygen isotope measurements using the SIMS method resulted in spot-to-spot reproducibility of 0.3‰ (2σ) during the analytical run, and individual spot analyses typically had errors of 0.5‰ (2σ). The oxygen isotope ratios $\delta^{18}\text{O}$ (reported relative to Vienna standard mean ocean water or VSMOW) are presented in Table 2. A summary of the results for each grain, along with characteristics of that grain are shown in Table 3. The complete SIMS oxygen isotope analytical results for the Orosmayo sapphires and PAR-1 ruby are given in Supplementary Materials Table S1. There was large variation between the different grains analyzed, overall from +4.1 to +11.2 $\delta^{18}\text{O}$ ‰, and a measurable variation within sample AC-3 up to 1.6‰ (Table 3). Although this variation is caused by the one outlier point (spot 3, also see Figure 3), sample AC-1 also showed a variation of 1.5‰ without any clear outliers (Table 3). There was no consistent zonation in terms of core to rim variation amongst the sapphires analyzed. This would suggest much more complex growth mechanisms than simply from core to rim, which is also suggested by the occurrence of complex sector-zoned sapphires and these have the highest oxygen isotope values. Other methods, such as a detailed cathodoluminescence study, would help in understanding the growth zonation and possible growth mechanisms. The lowest values correspond to apparently unzoned blue sapphires and the highest values mostly occur within sector zoned sapphires.

Table 2. $\delta^{18}\text{O}$ oxygen isotope results for grains AC-1 to AC-5, and AC-7, AC-10 to AC-11, AC-13 to AC-16.

Sapphire	Analysis Point	$\delta^{18}\text{O}$	2σ abs	Part of Crystal
AC-1	1	8.66	0.49	outer core
	2	7.52	0.49	outer rim
	3	7.66	0.47	outer rim
	4	8.08	0.48	outer rim
	5	8.97	0.46	inner rim
AC-2	1	5.24	0.48	outer rim
	2	5.68	0.50	outer rim
	3	5.76	0.46	outer core
	4	5.41	0.48	inner core
	5	5.43	0.46	outer core
	6	5.5	0.48	outer rim
AC-3	1	5.77	0.48	inner rim
	2	5.28	0.58	outer core
	3	4.12	0.50	inner rim
	4	5.61	0.48	outer rim
	5	5.4	0.46	outer rim
AC-4	1	5.69	0.51	inner rim
	2	5.33	0.49	inner rim
	3	4.97	0.48	outer rim
	4	5.89	0.49	outer core
	5	5.92	0.48	outer rim
AC-5	1	7.8	0.45	outer rim
	2	8.42	0.45	outer rim
	3	8.05	0.46	outer rim
	4	7.52	0.47	outer core
	5	8.71	0.47	outer rim
AC-7	1	6.09	0.45	outer rim
	2	5.42	0.46	outer rim
	3	6.14	0.50	inner rim
	4	6.02	0.47	inner rim
	5	6.81	0.47	inner rim
	6	5.42	0.49	inner rim
	7	6.59	0.46	inner rim
	8	6.66	0.47	inner rim
	9	5.56	0.51	inner rim
	10	5.47	0.48	inner rim
AC-10	1	9.28	0.46	inner rim
	2	9.42	0.46	inner rim
	3	9.44	0.45	inner rim
	4	9.02	0.46	inner rim
	5	9.28	0.45	inner rim
	6	8.95	0.47	inner rim
	7	9.27	0.45	inner rim
	8	9.21	0.46	inner rim
	9	9.02	0.45	inner rim
AC-11	1	11.22	0.46	inner rim
	2	10.94	0.45	outer rim
	3	10.88	0.46	outer core
	4	11.21	0.45	inner core
	5	10.65	0.46	inner rim
AC-13	1	5.68	0.44	outer rim
	2	5.46	0.48	inner rim
	3	5.97	0.46	outer core
	4	5.91	0.45	outer core
	5	5.96	0.45	outer rim
AC-14	1	6.18	0.47	outer rim
	2	6.23	0.47	outer core
	3	6.51	0.44	core
	4	6.68	0.48	core
	5	6.29	0.44	outer rim
AC-15	1	9.38	0.45	outer rim
	2	9.57	0.47	inner rim
	3	9.36	0.46	outer core
	4	8.91	0.45	outer core
	5	9.36	0.43	outer rim
AC-16	1	9.18	0.48	outer rim
	2	8.84	0.45	outer core
	3	8.65	0.45	outer core
	4	8.94	0.46	inner rim
	5	9.00	0.44	outer rim

Table 3. Summary of $\delta^{18}\text{O}$ results for the 12 samples analyzed.

Sapphire	Range	Range Variation	Average	Characteristics
AC-1	7.52–8.97	1.45	8.18	star sapphire
AC-2	5.24–5.76	0.52	5.50	magmatic zoning
AC-3	4.12–5.77	1.65	5.24	blue sapphire
AC-4	4.97–5.92	0.95	5.56	sector zoning
AC-5	7.52–8.71	1.19	8.10	blue-lilac
AC-7	5.42–6.81	1.39	6.02	pale lilac
AC-10	8.95–9.44	0.49	9.21	blue-lilac
AC-11	10.65–11.22	0.57	10.98	sector zoning
AC-13	5.46–5.97	0.51	5.80	deep blue
AC-14	6.18–6.68	0.50	6.38	sector zoning
AC-15	8.91–9.57	0.66	9.32	star sapphire
AC-16	8.65–9.18	0.53	8.92	sector zoning

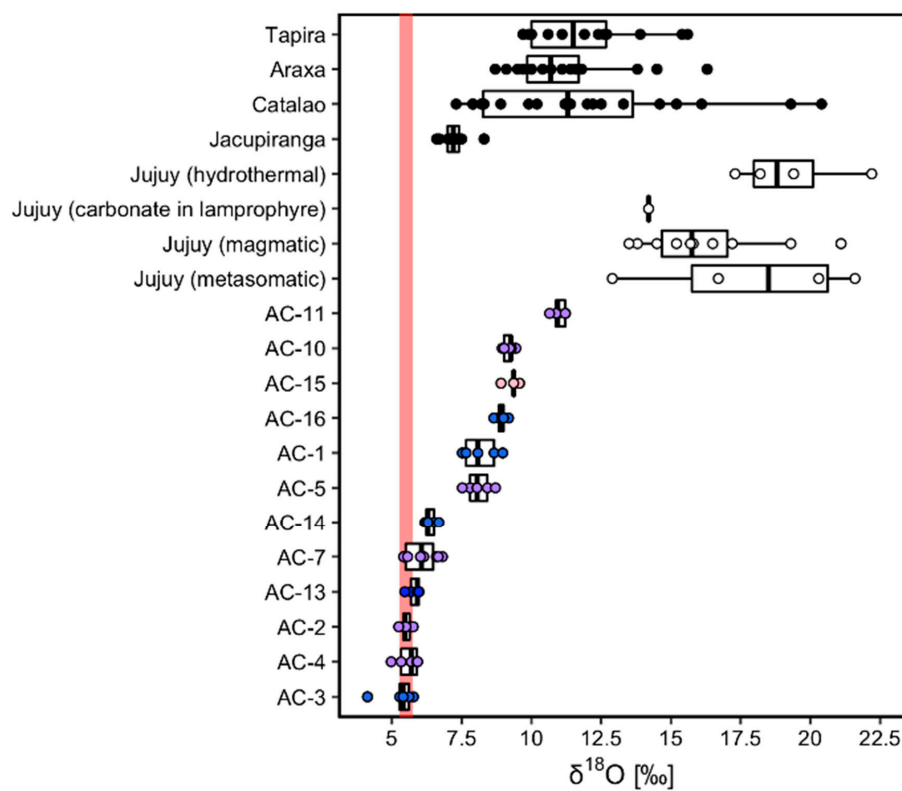


Figure 3. Diagram showing the range in oxygen isotope values for Jujuy sapphires (this study) in comparison to carbonatites and lamprophyres from the Jujuy region [17] and those of carbonatites from Brazil [18] and mantle $\delta^{18}\text{O}$ value (red band).

4. Discussion

4.1. Oxygen Isotope Groupings

Although there is a continuous spectrum in terms of trace element chemistry and $\delta^{18}\text{O}$ values, five main groupings are apparent: Group 1 ($n = 4$) comprises the blue sapphires and has $\delta^{18}\text{O}\text{‰}$ 4.1–5.9; Group 2 ($n = 2$) comprises pale lilac-blue sapphires with $\delta^{18}\text{O}\text{‰}$ 5.4–6.7; Group 3 ($n = 2$) consists of one star sapphire (AC-1) and a blue-lilac sapphire (AC-5) with $\delta^{18}\text{O}\text{‰}$ 7.5–8.9; Group 4 ($n = 3$) comprises a pale blue sapphire (AC-10), a star sapphire (AC-15) and a sector zone colorless-blue sapphire (AC-16) with $\delta^{18}\text{O}\text{‰}$ 8.6–9.6 and Group 5 ($n = 1$) is a sector zoned colorless-blue sapphire (AC-11) with $\delta^{18}\text{O}\text{‰}$ 10.6–11.2. These groupings, along with a summary of their trace element chemistry based on

Harris et al. (2017) [15] are shown in Table 4. Collectively, there is a range in $\delta^{18}\text{O}$ from 4.1‰ to 11.2‰ and a range in Ga/Mg of 0.3–10.4 (average range of 0.73–7.7) but no correlation or apparent relationship between Ga/Mg and the oxygen isotope values. Importantly, Baldwin et al. (2017) [19] found that sapphire megacrysts from the Siebenbirge Volcanic Field of Germany had a wide Ga/Mg of 1.0–23.4 and ascribed this to the influence of a carbonatitic melt in the crystallization of the sapphires. The range in Ga/Mg values for Jujuy Province sapphires at 0.30–10.40 fits well within this range and, based on this alone, would tentatively suggest a similar mechanism of formation. However, interpretation of Ga/Mg ratios in sapphires must be treated with caution as Sutherland et al. (2009) [20] found an even larger range in Ga/Mg for Australian basalt-hosted blue-green-yellow (BGY suite) sapphires with 0.24–31.60 for the Yarrowitch field and 0.17–193 for the Barrington field. This collectively lends support to the views of Baldwin et al. (2017) [19] and Palke et al. (2017) [21] who suggested that Ga/Mg ratios are not good discriminators for sapphire origin.

Table 4. Groupings based on $\delta^{18}\text{O}$ ‰ compositions with their main geochemical characteristics from Harris et al. (2017) [15].

Group 1 (Blue Sapphires) with $\delta^{18}\text{O}$ ‰ from 4.12 to 5.92									
Sapphire	Mg	Ti	V	Cr	Fe	Ga	Fe/Mg	Ga/Mg	Number of analyses
AC-2	38	73	64	456	789	140	22.3	4	6
AC-3	119	1987	154	359	1024	118	9.8	1.2	5
AC-4	103	1771	230	160	843	126	9.5	1.4	4
AC-13	162	428	155	91	1481	119	9.3	0.73	4
Group 2 (Pale Blue-Lilac Sapphires) with $\delta^{18}\text{O}$ ‰ from 5.42 to 6.68									
Sapphire	Mg	Ti	V	Cr	Fe	Ga	Fe/Mg	Ga/Mg	Number of analyses
AC-7	87	1044	113	224	621	116	7.8	1.5	4
AC-14	20	190	16	27	1348	121	86	7.7	4
Group 3 (Star Sapphire AC-1; Blue-Lilac Sapphire AC-5) with $\delta^{18}\text{O}$ ‰ from 7.52 to 8.97									
Sapphire	Mg	Ti	V	Cr	Fe	Ga	Fe/Mg	Ga/Mg	Number of analyses
AC-1	259	6619	187	45	927	146	4.3	0.8	6
AC-5	42	1077	67	209	677	99	17.3	2.5	4
Group 4 (Pale Blue Sapphire AC-10; Star Sapphire AC-15; Sector Zoned Colorless to Blue Sapphire AC-16) with $\delta^{18}\text{O}$ ‰ from 8.65 to 9.57									
Sapphire	Mg	Ti	V	Cr	Fe	Ga	Fe/Mg	Ga/Mg	Number of analyses
AC-10	71	1037	76	89	777	105	11	1.5	4
AC-15	200	6831	163	309	1278	160	6.5	0.8	4
AC-16	38	348	63	202	581	99	17	2.9	4
Group 5 (Sector Zoned Colorless to Blue Sapphire) with $\delta^{18}\text{O}$ ‰ from 10.65 to 11.22									
Sapphire	Mg	Ti	V	Cr	Fe	Ga	Fe/Mg	Ga/Mg	Number of analyses
AC-11	106	1741	230	16	517	128	5	1.3	4

4.2. What Do the Oxygen Isotopes Tell Us about the Primary Source for Jujuy Sapphires?

A framework on the interpretation of the geological origin of gem corundums using the $^{18}\text{O}/^{16}\text{O}$ ratio first proposed by Giuliani et al. (2005) [1] is now widely adopted. Based on this framework, rubies and pink sapphires can be classified into 5 categories based on their $\delta^{18}\text{O}$ value range. 1. Mafic gneiss hosted 2.9–3.8‰; 2. Mafic-ultramafic rocks (amphibolite, serpentinite) 3.2–6.8‰; 3. Desilicated pegmatites 4.2–7.5‰; 4. Shear zones cross-cutting ultramafic lenses and pegmatites within sillimanite gneisses 11.9–13.1‰; 5. Marble-hosted rubies 16.3–23‰. This framework has been further validated by numerous subsequent corundum oxygen isotope studies [3–5,11,13,20,22–32]. A summary of worldwide oxygen isotope values for gem sapphires, along with their host rock and Ga/Mg ratios, is presented in Table 5. In a study of sapphires from the French Massif Central basaltic field, Giuliani et al. (2009) [25] found two distinctive groups. The first group with $\delta^{18}\text{O}$ from 4.4‰ to 6.8‰ were believed to have crystallized from felsic magmas in the upper mantle while the second group with higher $\delta^{18}\text{O}$ from 7.6‰ to 13.9‰ were believed to have been derived from lower crustal granulites. However, the oxygen isotope range for Jujuy sapphires spans across both of these groupings. Critically, the study of Harris et al. (2017) [15] showed that for Jujuy sapphires, there is a continuous spectrum

in composition with significant trace element variation within single grains. This strongly suggests crystallization from the same source but under variable metasomatic conditions.

Table 5. Summary of worldwide oxygen isotope ranges and Ga/Mg for some sapphires (n.d = not determined).

Color	Host Rock	$d^{18}O_{\text{‰}}$	Ga/Mg	Reference
Blue, yellow, brown	alkali basalts	4.6–5.2	5.7–11.3	[31]
Pink	kimberlites	4.3–5.4	1.9–3.9	[31]
Blue	lamprophyre	5.4–6.8	0.3–0.5	[21]
Blue, yellow, green, colorless, brown	alkali basalts	2.7–6.9	n.d	[29]
Blue, green, yellow	alkali basalts	4.5–5.6	3–18	[13]
Blue, grey-pink, pink	alkali basalts	3.8–5.9	0.9–4.8	[26]
Blue, violet	lamprophyre	4.5–7.7	0.2–0.6	[33]
Blue, green, pink, colorless	alkali basalts	4.4–6.8	n.d	[25]
Blue, green, grey, white	alkali basalts	7.6–13.9	n.d	[25]
Blue, grey, brown	alkali basalts	n.d	1.0–23.4	[19]
Blue, violet	alluvial	2.6–6.8	0.6–9.0	[34]
Blue, green	alkali basalts	4.3–6.4	n.d	[5]
Blue, grey, violet, red	syenite pegmatites	2.0–10.6	n.d	[5]
Blue, green, yellow	alkali basalts	1.34–39.29	5.3–5.4	[20]
Blue, green, yellow	alkali basalts	6.6–193.0	5.2–5.8	[20]
Blue, green, yellow, pink	alkali basalts	4.3–8.4	n.d	[1]
Blue, grey	amphibolite	4.2–4.9	n.d	[1]
Blue	desilicated pegmatite in mafic rocks	10.9–11.2	n.d	[1]
Yellow, green, colorless, brown	syenite/anorthoclase	5.2–7.8	n.d	[1]
Blue, grey, colorless	skarn	7.7–10.7	n.d	[1]

In a study of carbonatites from Brazilian alkaline complexes, Santos and Clayton (1995) [18] found that the non-fenitized carbonatites from Jacupiranga had significantly lower oxygen isotope ratios (6.6–7.3) compared to the fenitized (i.e., K and Na metasomatism; Elliott et al. 2018, [35]) carbonatites of Araxa (9.7–16.3), Catalao (7.3–19.3), and Tapira (9.7–15.4). Zappettini et al. (1998) [17] analyzed a range of carbonatites from Jujuy Province and found that oxygen isotope values for magmatic carbonatites (13.5–21.1), metasomatic carbonatites (12.9–21.6), and hydrothermally altered carbonatites (17.3–22.2) overlapped each other but that magmatic carbonatites had lower values in general. They also analyzed one carbonatized lamprophyre sample which gave a value of 14.2 within the field of the magmatic carbonatites. The range in oxygen isotope compositions for Jujuy sapphires is much lower than all of these analyzed carbonatites and the lamprophyre from this region [17]. However, Harmon et al. (1981) [36] analyzed volcanic rocks from Cerro Galan in Catamarca Province, 400 km to the south of Jujuy, and found that these calc-alkaline volcanics had a range in oxygen isotope values from 8.3 to 10.7, and had formed directly from mantle-derived magmas but with likely partial crustal assimilation during ascent. This range is well within that of Groups 3–5 from the Jujuy suite. Additionally, the Brazilian fenitized carbonatites have a very similar range and would tentatively suggest that there was significant metasomatic influence in the Jujuy sapphire-forming environment, especially for the sapphires with the highest oxygen isotope ratios (Figure 3). It also suggests influence from an additional underlying deep source that had lower values than those for the carbonatites previously analyzed from Jujuy Province. This metasomatic influence would have been highly variable, as suggested by the wide range in oxygen isotope ratios and trace element contents and ratios for the Jujuy sapphires as shown by Harris et al. (2017) [15].

As suggested by Baldwin et al. (2017) [19], a possible origin of sapphires from carbonatitic melts could be identified by undertaking oxygen isotope measurements on the sapphires as, in general, carbonate-associated sapphires generally have higher isotopic ratios [1], as seen for the higher range amongst the Jujuy sapphires. However, interpreting such data would be problematic as there are no data available on oxygen isotope fractionation between corundum and co-existing carbonatitic melt [19].

4.3. Origin of Jujuy Sapphires

Any model proposed for the genesis of the alluvial Jujuy sapphires needs to account for (1) a predominant metamorphic source signature, and a less prominent mafic-ultramafic association and contrasting felsic/acidic association; (2) elevated Si contents, and unusually high Ga content for metamorphic sapphires (i.e., typically >100); (3) enrichments in Be, Nb, Ta, Sn, Th, and U within syngenetic rutile growths; (4) elevated light rare earth element (LREE) concentrations; (5) a bimodal mineral inclusion suite, including sulfides, feldspar, phosphates, and likely LREE-bearing minerals; (6) the range in Ga/Mg from 0.88 to 7.33; (7) significant variation in trace element contents, ratios, and oxygen isotope ratios within single grains; and (8) a wide but continuous range in oxygen isotope values from 4.1‰ to 11.2‰.

Given the presence of LREE-bearing inclusions and elevated LREE concentrations, it is possible that these elevated contents were the result of a carbonatitic parental melt. This is possible given reports of REE-bearing carbonatites within Jujuy Province. Based on $\delta^{13}\text{C}$ and $\delta^{18}\text{O}$ isotopic studies, Zappettini et al. (1998) [17] suggested that these carbonatites formed by the crystallization of carbonate magma with subsequent formation of metasomatic and hydrothermal carbonatitic veins. This is akin to the variably fenitized carbonatites from Brazil as shown above. Similarly, nearby Rio Grande monchiquites (163 ± 9 Ma) were shown to have been derived from heterogeneous enriched lithospheric mantle metasomatized by carbonatite fluids involving significant magma mixing (Hauser et al. 2010) [37]. Similar processes, involving exchanges between a carbonatite (Si-poor) and mantle-derived acidic magma (Si- and Ga-rich) could, in turn, be responsible for sapphire-bearing lamprophyre formation (e.g., the plumasite model; Peucat et al. 2007) [38] within Jujuy Province (e.g., Zappettini 1989) [39]. Factor analysis on Jujuy sapphires by Harris et al. (2017) [15] showed a largely continuous linear grouping from the metasomatic field of Giuliani et al. (2014) [4] into their plumasite field. The one exception to this trend was the star sapphires (i.e., the sapphires with the highest oxygen isotope ratios) which formed a distinctly separate grouping within the plumasite field of Giuliani et al. (2014) [4]. This once again provides supporting evidence for a sapphire-crystallization environment involving highly variable metasomatic interaction.

Collectively, the in situ study of Harris et al. (2017) [15] and this in situ study provide crucial evidence for understanding the origin of Jujuy sapphires. Based on their study of surface features, mineral inclusions, and major and trace element chemistry, Harris et al. (2017) [15] concluded that the Jujuy sapphires crystallized via metasomatic fluid exchange between an evolved crustal felsic system and intruding coeval mantle-derived carbonatized lamprophyres as part of a regional-wide alkaline magmatic event within NW Argentina during the Lower Cretaceous. Oxygen isotope ratios for the Jujuy sapphires largely support this model but allow us to go one step further and suggest that the influence of carbonatites on sapphire crystallization was greater than previously thought, and that the localized sapphire-former crustal environment was more complex, involving episodic interactions between mantle-derived lamprophyres, mantle-derived carbonatites, lower crustal felsic magmas and, most likely, both mantle and lower crustal metasomatic fluids. As stated by Harris et al. (2017) [15], such a complex interplay of widely diverse magma and fluid compositions would induce localized desilicification reactions that would lead to localized sapphire crystallization. Based on all of the available evidence, we suggest that most of these interactions would have occurred at the crust/mantle boundary, with initial crystallization within the upper mantle (i.e., sapphires with lower oxygen isotope signatures of 4.12–6.50) then continuing crystallization within the lower crust (i.e., sapphires with oxygen isotope signatures >6.50).

The wide range in chemistry and oxygen isotope compositions but within a single comagmatic group is explained by the degree and type of interaction (i.e., carbonatite–lamprophyre vs. carbonatite–granite) between these magmas/fluids, with some crystallizing at lower crustal levels as suggested by Palke et al. [21,34] for sapphires from Montana, USA. The large within-grain variation seen in trace element contents, trace element ratios, and oxygen isotope ratios is highly suggestive

of a geochemically dynamic environment with rapidly changing degrees of interaction between the various diverse fluid and magmatic components, as described above.

This model accounts for the dominant metasomatic signature, while also accounting for the mafic–ultramafic (i.e., carbonatitic and lamprophyric magmas) and felsic (i.e., mantle-derived enriched acidic magmas and/or granitic anatectic melts) associations. It also accounts for the bimodal mineral inclusion suite, enrichment in LREE, Ga/Mg ratios, and range in trace element and oxygen isotope compositions within a single sapphire group that crystallized at the same time but across the crust–mantle boundary. The oxygen isotope values and range provide additional support to the initial hypothesis of Zappettini et al. (1997) [40], who proposed that the Jujuy sapphires formed via metasomatic exchanges between REE-bearing carbonatites and an evolved felsic magma during the Cretaceous (150–110 Ma), and were then subsequently incorporated as xenocrysts within lamprophyre dykes.

5. Conclusions

In situ SIMS oxygen isotope analyses on the Orosmayo sapphire suite revealed that they have values spanning a continuous range from +4.1 to +11.2 $\delta^{18}\text{O}\text{‰}$, with measurable variation within individual sapphires. Based on their trace element geochemistry, geochemical ratios, and oxygen isotopes, although there is a continuous spectrum of compositions, the sapphires can be subdivided into five suites reflecting different degrees of interaction between the various fluid/magmatic components involved in sapphire formation. Both the previous geochemical work and this study suggest that the Jujuy sapphires crystallized through the crust–mantle boundary in a localized environment involving episodic interactions between mantle-derived lamprophyres, mantle-derived carbonatites, lower crustal felsic magmas and, most likely, both mantle and crustal metasomatic fluids. This complex interplay of widely diverse magma and fluid compositions would induce localized desilicification reactions, leading to localized sapphire crystallization. This study reinforces the importance of carbonatites on sapphire crystallization. The significant range in trace element chemistry and oxygen isotope ratios within individual grains stresses the critical importance of undertaking in situ analysis on gem corundums in order to fully understand their environment of formation and to aid in their geographic typing.

Supplementary Materials: The following are available online at <http://www.mdpi.com/2075-163X/9/7/390/s1>, Table S1: Secondary Ion Mass Spectrometry (SIMS) Results.

Author Contributions: I.T.G. wrote the manuscript, was responsible for the conception of this project and interpreted the results of the analyses. S.J.H. provided input into the discussion and constructed some of the figures. L.M. Provided technical input and ran the SIMS analyses. A.L. provided technical input. E.Z. collected the samples and provided geological expertise on the Jujuy region of NW Argentina.

Funding: This research received no external funding.

Acknowledgments: The authors would like to thank Joanne Wilde, formerly of the School of BEES, for making the polished mounts required for SIMS analysis. The authors acknowledge the facilities and the scientific and technical assistance of the Australian Microscopy & Microanalysis Research Facility at the Centre for Microscopy, Characterisation & Analysis, The University of Western Australia, a facility funded by the University, State and Commonwealth Governments.

Conflicts of Interest: The authors declare no conflict of interest.

References

1. Giuliani, G.; Fallick, A.E.; Garnier, V.; France-Lanord, C.; Ohnenstetter, D.; Schwarz, D. Oxygen isotope composition as a tracer for the origins of rubies and sapphires. *Geology* **2005**, *33*, 249–252. [CrossRef]
2. Yui, T.-F.; Wu, C.-M.; Limtrakun, P.; Sricharin, P.; Boonsoong, A. Oxygen isotope studies on placer sapphires and ruby in the Chanthaburi-Trat alkali basalt gem field, Thailand. *Lithos* **2006**, *86*, 197–211. [CrossRef]
3. Giuliani, G.; Ohnenstetter, D.; Garnier, V.; Fallick, A.E.; Rakotondrazafy, M.; Schwarz, D. The geology and genesis of gem corundum deposits. In *Geology of Gem Deposits*; Groat, L.A., Ed.; Mineralogical Association of Canada: Quebec City, QC, Canada, 2007; Volume 37, pp. 23–78. ISBN 978092194375.

4. Giuliani, G.; Ohnenstetter, D.; Fallick, A.E.; Groat, L.; Fagan, J. The geology and genesis of gem corundum deposits. In *Geology of Gem Deposits (2nd edition)*; Groat, L.A., Ed.; Mineralogical Association of Canada: Quebec City, QC, Canada, 2014; Volume 44, pp. 29–112. ISBN 9780921294542.
5. Vysotskiy, S.V.; Nechaev, V.P.; Kissin, A.Y.; Yakovenko, V.V.; Ignat'ev, A.V.; Velivetskaya, T.A.; Sutherland, F.L.; Agoshkov, A.I. Oxygen isotopic composition as an indicator of ruby and sapphire origin: A review of Russian occurrences. *Ore Geol. Rev.* **2015**, *68*, 164–170. [[CrossRef](#)]
6. Yui, T.F.; Zaw, K.; Limtrakun, P. Oxygen isotope composition of the Denchai sapphire, Thailand: A clue to its enigmatic origin. *Lithos* **2003**, *67*, 153–161. [[CrossRef](#)]
7. Bindeman, I.N.; Schmitt, A.K.; Evans, D.A.D. Limits of hydrosphere-lithosphere interaction: Origin of the lowest-known $\delta^{18}\text{O}$ silicate rock on Earth in the Paleoproterozoic Karelian rift. *Geology* **2010**, *38*, 631–634. [[CrossRef](#)]
8. Bindeman, I.N.; Serebryakov, N.S. Geology, Petrology and O and H isotope geochemistry of remarkably ^{18}O depleted Paleoproterozoic rocks of the Belomorian Belt, Karelia, Russia, attributed to global glaciation 2.4 Ga. *Earth Planet. Sci. Lett.* **2011**, *306*, 163–174. [[CrossRef](#)]
9. Krylov, D.P. $^{18}\text{O}/^{16}\text{O}$ ratios in the corundum-bearing rocks of Khitostrov, northern Karelia. *Dokl. Earth Sci.* **2008**, *419*, 453–456. [[CrossRef](#)]
10. Sutherland, F.L.; Graham, I.T.; Harris, S.J.; Coldham, T.; Powell, W.; Belousova, E.A.; Martin, L. Unusual ruby-sapphire transition in alluvial megacrysts, Cenozoic basaltic gem field, New England, New South Wales, Australia. *Lithos* **2017**, *278*, 347–360. [[CrossRef](#)]
11. Wang, K.K.; Graham, I.T.; Martin, L.; Voudouris, P.; Giuliani, G.; Lay, A.; Harris, S.J.; Fallick, A.E. Fingerprinting Paranesti rubies through oxygen isotopes. *Minerals* **2019**, *9*, 91. [[CrossRef](#)]
12. Sutherland, F.L.; Abduriyim, A. Geographic typing of gem corundum: A test case from Australia. *J. Gemmol.* **2009**, *31*, 203–210. [[CrossRef](#)]
13. Sutherland, F.L.; Coenraads, R.R.; Abduriyim, A.; Meffre, S.; Hoskin, P.W.O.; Giuliani, G.; Beattie, R.; Wuhler, R.; Sutherland, G.B. Corundum (sapphire) and zircon relationships, Lava Plains gem fields, NE Australia: Integrated mineralogy, geochemistry, age determination, genesis and geographical typing. *Mineral. Mag.* **2015**, *79*, 545–581. [[CrossRef](#)]
14. Zappettini, E.; Mutti, D. Zafiros de la Puna Argentina: Un Potencial recurso minero. *Recur. Miner.* **1997**, *2*, 33–62.
15. Harris, S.J.; Graham, I.T.; Lay, A.; Powell, W.; Belousova, E.; Zappettini, E. Trace element geochemistry and metasomatic origin of alluvial sapphires from the Orosmayo region, Jujuy Province, northwest Argentina. *Can. Mineral.* **2017**, *55*, 595–617. [[CrossRef](#)]
16. Chernicoff, C.J.; Richards, J.P.; Zappettini, E.O. Crustal lineament control on magmatism and mineralization in northwestern Argentina: Geological, geophysical, and remote sensing evidence. *Ore Geol. Rev.* **2002**, *21*, 127–155. [[CrossRef](#)]
17. Zappettini, E.O.; Rubiolo, D.; Hubberten, H.W. *Carbon and Oxygen Isotopes in Carbonatites from Puna, Jujuy and Salta, Argentina*; Congreso Nacional de Geología Económica: Buenos Aires, Argentina, 1998; Volume 2. (In Spanish)
18. Santos, R.V.; Clayton, R.N. Variations of oxygen and carbon isotopes in carbonatites: A study of Brazilian alkaline complexes. *Geochim. Cosmochim. Acta* **1995**, *59*, 1339–1352. [[CrossRef](#)]
19. Baldwin, L.C.; Tomaschek, F.; Ballhaus, C.; Gerdes, A.; Fonseca, R.O.C.; Wirth, R.; Geisler, T.; Nagel, T. Petrogenesis of alkaline basalt-hosted sapphire megacrysts: Petrological and geochemical investigations of in situ sapphire occurrences from the Siebengebirge Volcanic Field, Germany. *Contrib. Mineral. Petrol.* **2017**, *172*, 1–27. [[CrossRef](#)]
20. Sutherland, F.L.; Zaw, K.; Meffre, S.; Giuliani, G.; Fallick, A.E.; Graham, I.T.; Webb, G.B. Gem-corundum megacrysts from east Australian basalt fields: Trace elements, oxygen isotopes and origins. *Aust. J. Earth Sci.* **2009**, *56*, 1003–1022. [[CrossRef](#)]
21. Palke, A.; Renfro, N.D.; Berg, R.B. Melt inclusions in alluvial sapphires from Montana, USA: Formation of sapphires as a restitic component of lower crustal melting? *Lithos* **2017**, *278*, 43–53. [[CrossRef](#)]
22. Giuliani, G.; Fallick, A.E.; Rakotondrazafy, M.; Ohnenstetter, D.; Andriamamonjy, A.; Rakotosamizanany, S.; Ralantoarison, T.; Razanatseheno, M.; Dunaigre, C.; Schwarz, D. Oxygen isotope systematics of gem corundum deposits in Madagascar: Relevance for their geological origin. *Miner. Depos.* **2007**, *42*, 251–270. [[CrossRef](#)]

23. Sutherland, F.L.; Duroc-Danner, J.M.; Meffre, S. Age and origin of gem corundum and zircon megacrysts from the Mercaderes–Rio Mayo area, South-west Colombia, South America. *Ore Geol. Rev.* **2008**, *34*, 155–168. [[CrossRef](#)]
24. Garnier, V.; Giuliani, G.; Ohnenstetter, D.; Fallick, A.E.; Dubessy, J.; Banks, D.; Vinh, H.Q.; Lhomme, T.; Maluski, H.; Pecher, A.; et al. Marble-hosted ruby deposits from central and southeast Asia: Towards a new genetic model. *Ore Geol. Rev.* **2008**, *34*, 169–191. [[CrossRef](#)]
25. Giuliani, G.; Fallick, A.; Ohnenstetter, D.; Pegere, G. Oxygen isotopes compositions of sapphires from the French Massif Central: Implications for the origin of gem corundum in basaltic fields. *Miner. Depos.* **2009**, *44*, 221–231. [[CrossRef](#)]
26. Uher, P.; Giuliani, G.; Szakall, S.; Fallick, A.; Strunga, V.; Vaculovic, T.; Ozdin, D.; Greganova, M. Sapphires related to alkali basalts from the Cerova Highlands, Western Carpathians (southern Slovakia): Composition and origin. *Geol. Carpathica* **2012**, *63*, 71–82. [[CrossRef](#)]
27. Vysotskiy, S.V.; Ignat'ev, A.V.; Levitskii, V.I.; Nechaev, V.P.; Velvetskaya, T.A.; Yakovenko, V.V. Geochemistry of stable oxygen and hydrogen isotopes in minerals and corundum-bearing rocks in Northern Karelia as an indicator of their unusual genesis. *Geochem. Int.* **2014**, *52*, 773–782. [[CrossRef](#)]
28. Sutherland, F.L.; Zaw, K.; Meffre, S.; Yui, T.F.; Thu, K. Advances in trace element “fingerprinting” of gem corundum, ruby and sapphire, Mogok Area, Myanmar. *Minerals* **2014**, *5*, 61–79. [[CrossRef](#)]
29. Rakotosamizanany, S.; Giuliani, G.; Ohnenstetter, D.; Rakotondrazafy, A.F.M.; Fallick, A.E.; Paquette, J.-L.; Tiepolo, M. Chemical and oxygen isotopic compositions, age and origin of gem corundums in Madagascar alkali basalts. *J. Afr. Earth Sci.* **2014**, *94*, 156–170. [[CrossRef](#)]
30. Zaw, K.; Sutherland, L.; Yui, T.F.; Meffre, S.; Thu, K. Vanadium-rich ruby and sapphire within Mogok Gemfield, Myanmar: Implications for gem color and genesis. *Miner. Depos.* **2015**, *50*, 25–39. [[CrossRef](#)]
31. Giuliani, G.; Pivin, M.; Fallick, A.E.; Ohnenstetter, D.; Song, Y.; Demaiffe, D. Geochemical and oxygen isotope signatures of mantle corundum megacrysts from the Mbuji-Mayi kimberlite, democratic Republic of Congo, and the Changle alkali basalt, China. *Comptes Rendus Geosci.* **2015**, *347*, 24–34. [[CrossRef](#)]
32. Wong, J.; Verdel, C. Tectonic environments of sapphire and ruby revealed by a global oxygen isotope compilation. *Int. Geol. Rev.* **2018**, *60*, 188–195. [[CrossRef](#)]
33. Palke, A.C.; Wong, J.; Verdel, C.; Avila, J.N. A common origin for Thai/Cambodian rubies and blue and violet sapphires from Yogo Gulch, Montana, U.S.A.? *Am. Mineral.* **2018**, *103*, 469–479. [[CrossRef](#)]
34. Palke, A.C.; Renfro, N.D.; Berg, R.B. Origin of sapphires from a lamprophyre dike at Yogo Gulch, Montana, USA: Clues from their melt inclusions. *Lithos* **2016**, *260*, 339–344. [[CrossRef](#)]
35. Elliott, H.A.L.; Wall, F.; Chakhmouradian, A.R.; Siegfried, P.R.; Dahlgren, S.; Weatherley, S.; Finch, A.A.; Marks, M.A.W.; Dorman, E.; Deady, E. Fenites associated with carbonatite complexes: A review. *Ore Geol. Rev.* **2018**, *93*, 38–59. [[CrossRef](#)]
36. Harmon, R.S.; Thorpe, R.S.; Francis, P.W. Petrogenesis of Andean andesites from combined O-Si isotope relationships. *Nature* **1981**, *290*, 396–399. [[CrossRef](#)]
37. Hauser, N.; Matteini, M.; Omarini, R.H.; Pimentel, M.M. Constraints on metasomatised mantle under Central South America: Evidence from Jurassic alkaline lamprophyre dykes from the Eastern Cordillera, NM Argentina. *Mineral. Petrol.* **2010**, *100*, 153–184. [[CrossRef](#)]
38. Peucat, J.J.; Ruffault, P.; Fritsch, E.; Bouhnik-La Coz, M.; Simonet, C.; Lasnier, B. Ga/Mg ratios as a new geochemical tool to differentiate magmatic from metamorphic blue sapphire. *Lithos* **2007**, *98*, 261–274. [[CrossRef](#)]
39. Zappettini, E. Geología y Metalogénesis de la Región Compreendida Entre las Localidades de Santa Ana y Cobres, Provincias de Jujuy y Salta, República Argentina. Ph.D. Thesis, Facultad de Ciencias Exactas y Naturales, Universidad de Buenos Aires, Buenos Aires, Argentina, 1989.
40. Zappettini, E.; Mutti, D.; Bernhardt, H.J. Genesis de Zafiro y hercinita de la puna argentina. *Actas* **1997**, *2*, 1598–1602.

